**Observing Metal-catalyzed Chemical Reactions in situ using Surface-enhanced Raman Spectroscopy on Pd-Au Nanoshells**

Kimberly N. Heck, Benjamin G. Janesko, Gustavo E. Scuseria, Naomi J. Halas, Michael S. Wong

## Supplementary Information

### Description of DFT calculations on chemisorbed 1,1-DCE

All calculations were performed with a development version of the Gaussian electronic structure program [1]. Calculations use the B3LYP [2-5] density functional, with (unless noted otherwise) the LANL2DZ basis set and effective core potential [6-8] on Pd and the 6-31+G(d,p) basis on other atoms. Calculations use "Tight" convergence criteria for SCF iterations and geometry optimizations, and a pruned (99,590) "UltraFine" integration grid. No solvent model is included. All systems are assumed to be in the lowest possible spin state, and singlet calculations are spin-restricted. Spatial symmetry is ignored except where noted. Calculated vibrational frequencies are scaled by a factor of 0.98 as recommended in Ref. 9. Table S1 compares experimental (CCCBDB, Ref. 12) and calculated vibrational frequencies for 1,1-DCE evaluated using various basis sets. The 6-31+G(d,p) basis provides a reasonable compromise between accuracy and efficiency, with a mean absolute error (MAE) of 26 $cm^{-1}$ versus experiment. This is deemed sufficient for the desired semiquantitative interpretations of experiment.

Table S1: Calculated (B3LYP) and experimental vibrational frequencies of 1,1-DCE, and assignments.

| Symm | Assignment | Exptl | LANL2DZ | 6-31+G(d,p) | 6-311++G(3df,3pd) |
|---|---|---|---|---|---|
| A1 | C-H symmetric stretch | 3035 | 3127 | 3123 | 3109 |
| A1 | **C-C stretch** | 1627 | 1635 | 1635 | 1627 |
| A1 | **$CH_2$ bend** | 1400 | 1396 | 1380 | 1383 |
| A1 | C-Cl symmetric stretch | 603 | 533 | 585 | 588 |
| A1 | $CCl_2$ bend | 299 | 276 | 296 | 295 |
| A2 | $CH_2$ twist | 686 | 675 | 676 | 686 |
| B1 | $CH_2$ wag | 875 | 931 | 875 | 897 |
| B1 | $CCl_2$ wag | 460 | 428 | 463 | 471 |
| B2 | C-H antisymmetric stretch | 3130 | 3236 | 3219 | 3203 |
| B2 | C-C-H bend, C-Cl stretch | 1095 | 1079 | 1073 | 1080 |
| B2 | C-Cl antisymmetric stretch | 800 | 706 | 755 | 756 |
| B2 | Cl-C-C bend | 372 | 357 | 373 | 374 |
| MAE | -- | -- | 44 | 26 | 23 |

Table S2 presents calculated frequencies of the Raman-active C-C stretch and $CH_2$ bend vibrational modes of 1,1-DCE and various substitution products bound to Pd clusters. These vibrational modes are marked in bold in Table S1. (All calculated modes involve some coupling between C-C stretching and $CH_2$ bending, and are tabulated based on the dominant contribution.) The calculated Raman activities (not shown) are always appreciable for both modes. The C-C stretch frequency has previously been shown to provide a sensitive probe of ethylene adsorption geometry [10]. We find that the C-C stretch frequency dramatically decreases as DCE goes from free, to π-bound, to di-σ-bound, while the $CH_2$ bend frequency is not significantly affected. The intense SERS peaks seen experimentally below ~1200 $cm^{-1}$ are most consistent with di-σ-coordinated DCE.

The calculated vibrational frequencies of a mono-dechlorinated product obtained by replacing one Cl atom with Pd are rather strongly dependent on the cluster model. Neutral 1-chloro-1-palladio-ethylene is a radical with a Cl-C-Pd angle (121°) close to the

Cl-C-Cl angle in 1,1-DCE (114$^{o}$), and with C-C stretch and $CH_2$ bend frequencies similar to π-bound DCE. In contrast, the corresponding closed-shell cation has a much smaller Cl-C-Pd angle (93$^{o}$), and C-C stretch and $CH_2$ bend frequencies similar to gas-phase DCE. The calculated Raman spectra (not shown) have several other intense peaks below 1000 wavenumber, suggesting that the mono-dechlorinated product may be rather uncommon in the experimental spectra. Calculations on monodechlorinated DCE on larger Pd cluster models tended to converge to geometries with dissociated C-Cl bonds, providing additional evidence that the monodechlorinated product is unstable.

The vibrational spectrum of fully dechlorinated vinylidene ($C{=}CH_2$) bound to Pd also shows some dependence on the binding motif. A neutral two-atom Pd cluster gives neutral, closed-shell 1,1-di-palladio-ethylene, with calculated C-C stretch and $CH_2$ bend frequencies comparable to 1,1-DCE. We also explored vinylidene bound to atop, bridge, and threefold sites of a neutral tetrahedral $Pd_4$ cluster. The threefold site is most energetically stable, as seen by Clotet and coworkers [11], with bridge and atop sites calculated 12 and 45 kcal/mol higher in energy. The calculated C-C stretch frequency is significantly reduced for the threefold site, and significantly increased for the atop site. These calculations suggest that the Raman-active C-C stretch vibration of chemisorbed vinylidene may occur between 1350 and 1700 $cm^{-1}$, with the lower end corresponding to more highly coordinated (and presumably more realistic) models. The calculations also suggest that high-frequency modes 1800-2000 $cm^{-1}$ may correspond to $CH_2$ bending vibrations of surface-bound vinylidene.

Table S2: Selected vibrational frequencies calculated for adsorbates on Pd cluster models.

| System | C-C stretch | $CH_2$ bend |
|---|---|---|
| 1,1-DCE | 1635 | 1380 |
| Pd-DCE ($\pi$) | 1276 | 1452 |
| $Pd_2$-DCE (di-$\sigma$) | 1115 | 1405 |
| 1-chloro-1-palladio-ethylene | 1295 | 1480 |
| 1-chloro-1-palladio-ethylene(+) | 1654 | 1353 |
| 1,1-di-palladio-ethylene | 1617 | 1324 |
| $Pd_4$-vinylidene (bridge) | 1567 | 1340 |
| $Pd_4$-vinylidene (atop) | 1685 | 1288 |
| $Pd_4$-vinylidene (threefold) | 1382 | 2034 |

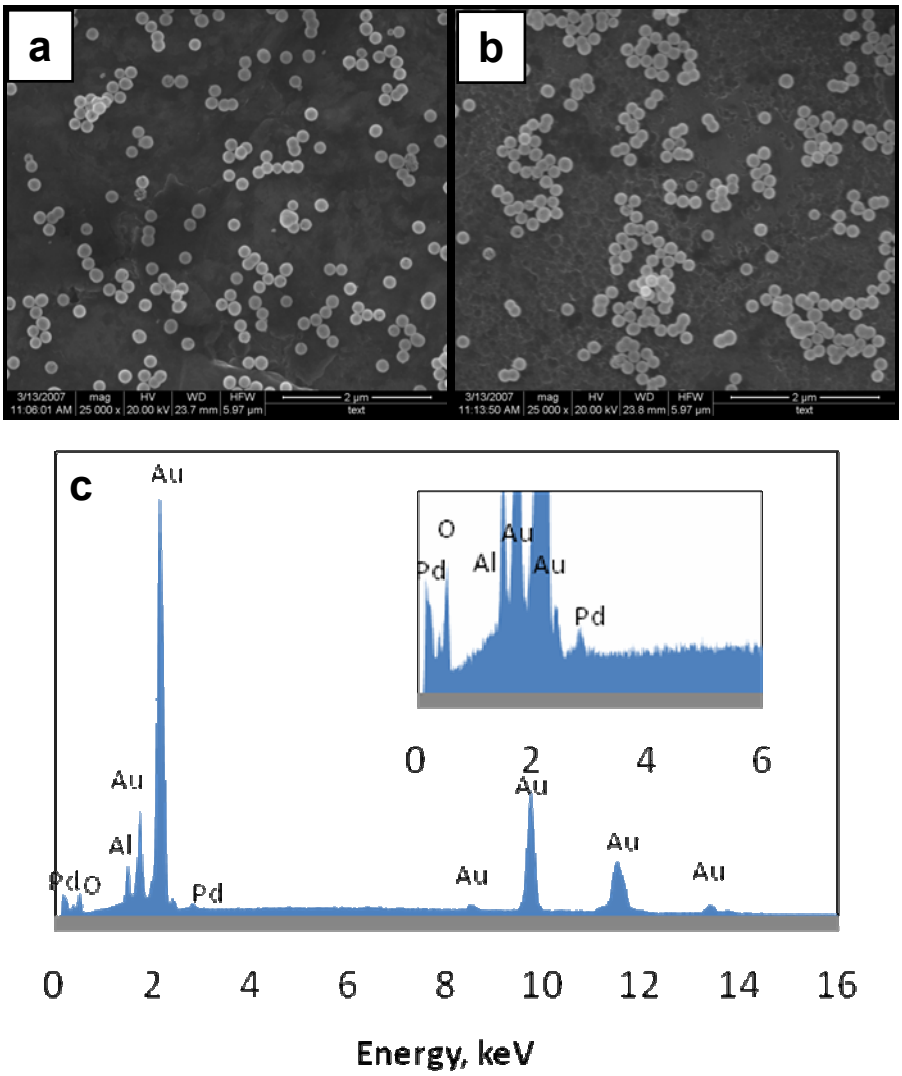


**Figure S1.** SEM images of (a) Au NSs and (b) Pd/Au NSs, and (c) EDS of Pd/Au NSs (Inset: Pd region).

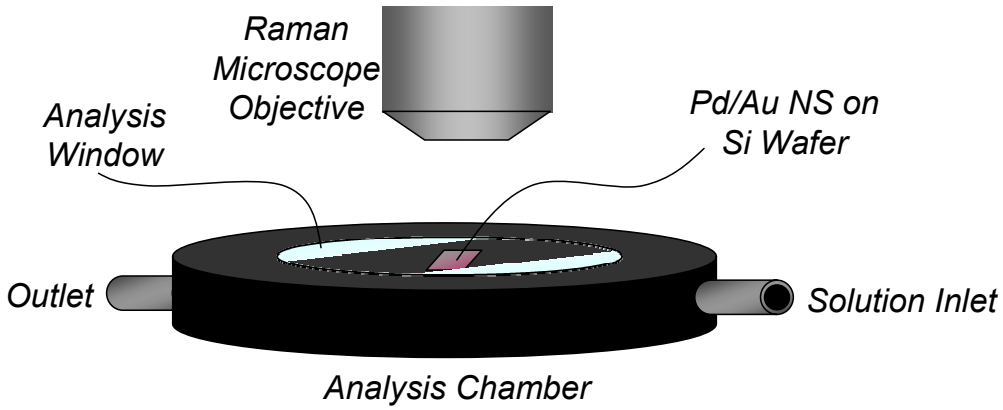


**Figure S2**. Schematic of flow chamber.

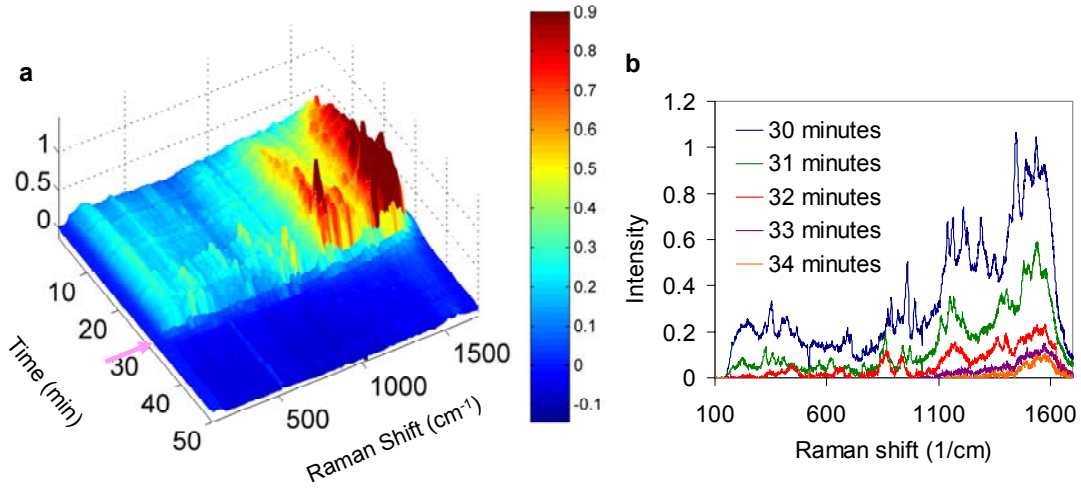


**Figure S3.** Waterfall plot of chemisorption of 254.4 μM 1,1-DCE followed by the addition of 81 mM $H_2$ in $H_2O$: (a) 1,1-DCE solution injected at t=0, $H_2$ in $H_2O$ added after 30 minutes, and (b) series of SERS spectra before and after addition of $H_2$ in $H_2O$.

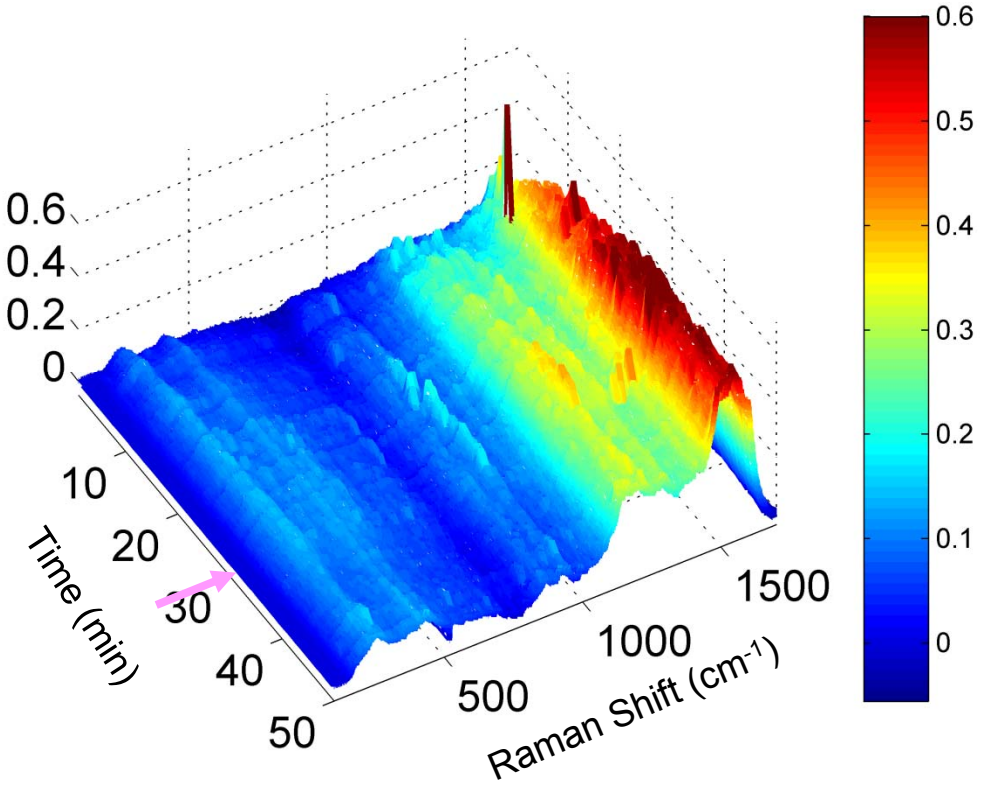


**Figure S4.** Waterfall plot of chemisorption of 254.4 μM 1,1-DCE followed by the addition of $N_2$ saturated water. 1,1-DCE solution injected at t=0, $N_2$ saturated water added after 30 minutes.

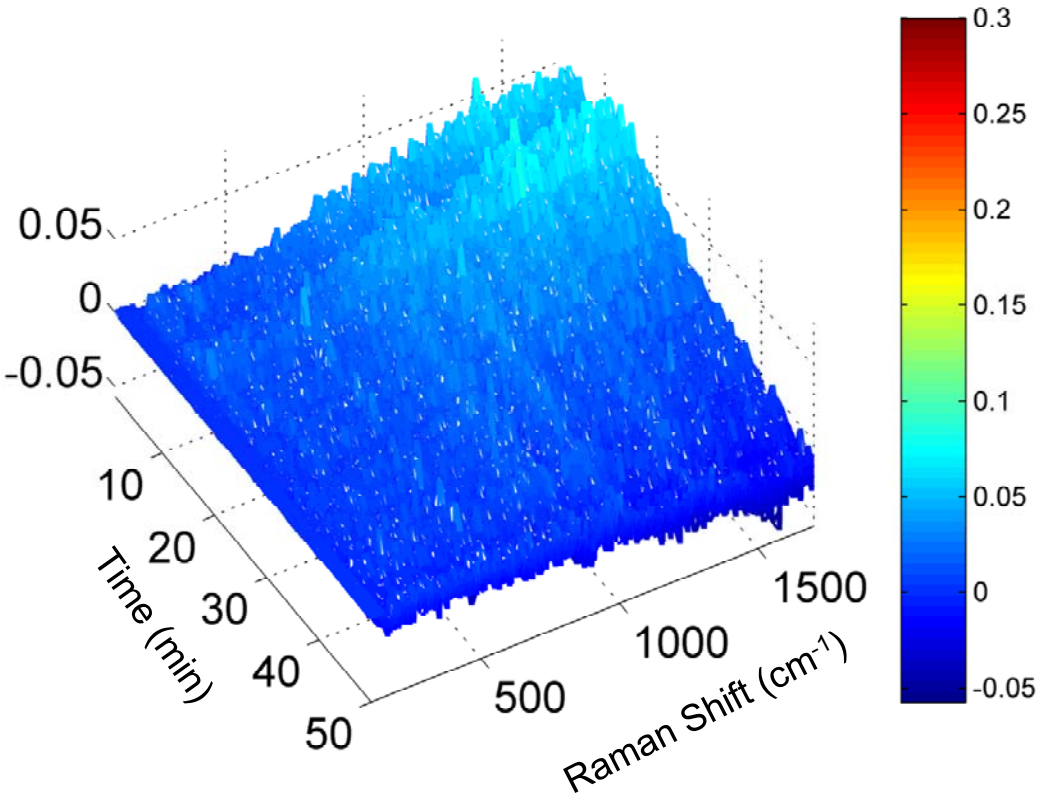


**Figure S5.** Waterfall plot of chemisorption of 254.4 μM 1,1-DCE over Au NSs.

**References**


1. Frisch, M. J., Trucks, G. W., Schlegel, H. B., Scuseria, G. E., *et al.*, *Gaussian Development Version, Revision F.02*, Gaussian, Inc.: Wallingford CT, 2006.
2. Stephens, P. J.; Devlin, F. J.; Chabalowski, C. F.; Frisch, M. J., *J. Phys. Chem.* **1994,** 98, 11623.
3. Becke, A. D., *J. Chem. Phys.* **1993,** 98, 5648.
4. Lee, C. T.; Yang, W. T.; Parr, R. G., *Phys. Rev. B* **1988,** 37, 785.
5. Vosko, S. H.; Wilk, L.; Nusair, M., *Can. J. Phys.* **1980,** 58, 1200.
6. Hay, P. J.; Wadt, W. R., *J. Chem. Phys.* **1985,** 82, 270.
7. Hay, P. J.; Wadt, W. R., *J. Chem. Phys.* **1985,** 82, 284.
8. Hay, P. J.; Wadt, W. R., *J. Chem. Phys.* **1985,** 82, 299.
9. Cardini, G.; Muniz-Miranda, M.; Pagliai, M.; Schettino, V., *Theor. Chem. Acc.* **2007,** 117, 451.
10. Stuve, E. M.; Madix, R. J., *J. Phys. Chem.* **1985,** 89, 3183.
11. Clotet, A.; Ricart, J. M.; Pacchioni, G., *J. Mo/. Struct. (THEOCHEM)* **1999,** 458, 123.
12. NIST Computational Chemistry Comparison and Benchmark DataBase, NIST Standard Reference Database Number 101, Release 14, September 2006, Editor: Russell D. Johnson III, http://srdata.nist.gov/cccbdb